The Alaskan Arctic Frontal Zone: Forcing by Orography, Coastal Contrast, and the Boreal Forest

AMANDA H. LYNCH

Program in Atmosphere and Ocean Sciences, and Cooperative Institute for Research in Environmental Sciences, University of Colorado, Boulder, Colorado

ANDREW G. SLATER

Department of Geography, University of Colorado, Boulder, Colorado

MARK SERREZE

Cooperative Institute for Research in Environmental Sciences, University of Colorado, Boulder, Colorado

(Manuscript received 9 October 2000, in final form 18 May 2001)

ABSTRACT

Experiments have been conducted with a regional climate model to indicate the conditions required to generate preferred regions of frontal activity in the Alaskan region. Several objective methods of frontal identification were first investigated. It was found that

- the vertical component of relative vorticity,
- a thermal front parameter $-\nabla|\nabla T_{850}| \cdot \mathbf{n}$, where T_{850} is the 850-hPa temperature and $\mathbf{n}$ is a unit vector in the direction of the 850-hPa temperature gradient, and
- a parameter derived from the **Q** vector as a measure of vertical motion

were useful in combination to determine the occurrence of fronts. The preferred locations for frontal activity were located to the southern side of the eastern Brooks Range and over the Alaska Range. These diagnostics were then used to characterize frontal frequency in a series of experiments removing topographic and vegetation contrasts. It was found that the removal of the treeline contrast and its associated heating gradient had a small effect on frontal frequency in the immediate vicinity of the tree line, but that the largest impact was in response to the removal of topography, greatly reducing frontal frequency. The coastal contrast was found to have a limited role in synoptic frontal activity in the Alaskan region.

1. Introduction

Conceptual models of the global general circulation typically have not included a separate high-latitude frontal zone. As noted by Serreze et al. (2001), the notion of a region of frequent mesoscale frontal activity in northern high latitudes emerging as distinct form of frontal activity in midlatitudes can be traced back to the early work of Dzerdzeevskii (1945). Reed and Kunkel (1960) termed this preferred region of frontal activity the ''Arctic frontal zone'' and like Dzerdzeevskii (1945), identified it as a summer phenomenon. By contrast, Bryson (1966) and Barry (1967) postulated that it is a year-round feature. Bryson (1966) in turn argued that its summer position may be responsible for determining the location of the northern tree line. As outlined in Serreze et al. (2001), disagreement regarding the seasonality of the Arctic frontal zone in large part arises from differences in study approaches. If one considers a priori that individual Arctic fronts represent the northernmost frontal boundaries observed, the Arctic frontal zone may be identified in any season. This approach is implicit in the study of Barry (1967). However, in compiling objective frontal frequency statistics based on any front observed, it is only in summer that a high-latitude frontal zone emerges that is distinct from midlatitude activity (Serreze et al. 2001).

The Arctic frontal zone has been proposed to arise from the differential heating between snow-free land and cold Arctic Ocean in summer, either alone or modified by orography (Dzerdzeevskii 1945; Reed and Kunkel 1960; Serreze et al. 2001); or, in a reversal of Bryson's (1966) reasoning, from contrasts in surface heating between the tundra and boreal forest (Hare and Ritchie 1972; Pielke and Vidale 1995).

Corresponding author address: Dr. Amanda H. Lynch, Cooperative Institute for Research in Environmental Sciences, University of Colorado, Boulder, CO 80309.
E-mail: manda@cires.colorado.edu

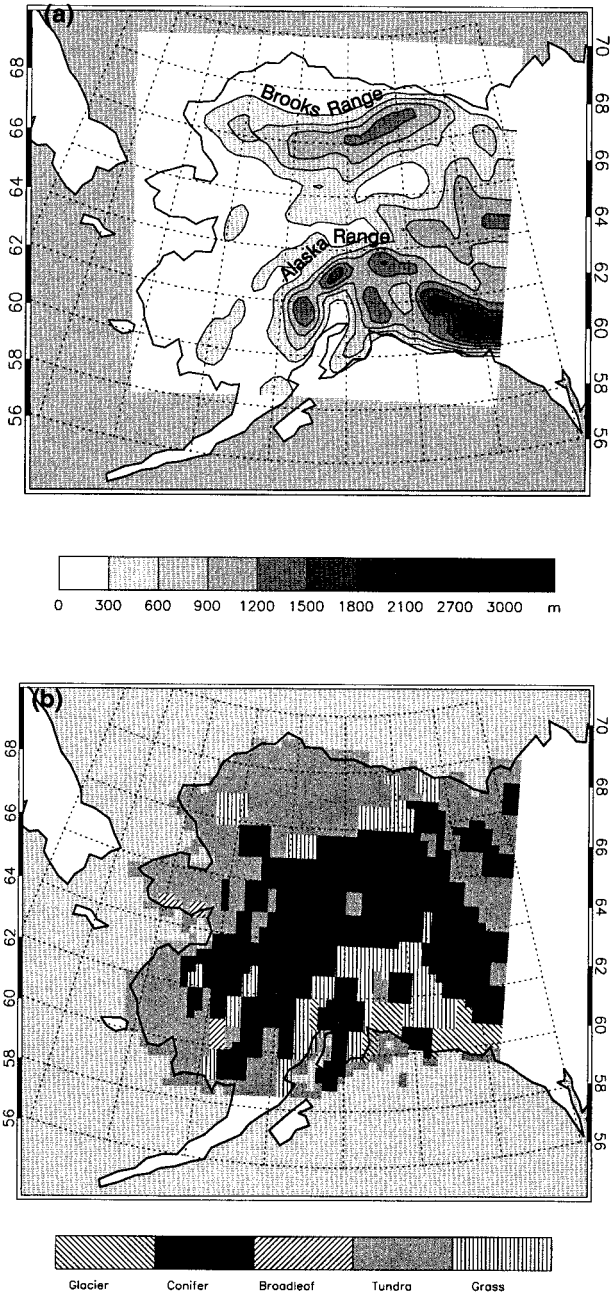

FIG. 1. (a) Alaskan domain at 30-km grid spacing, with topographic contours shown in meters. (b) Vegetation specification map for control simulation.

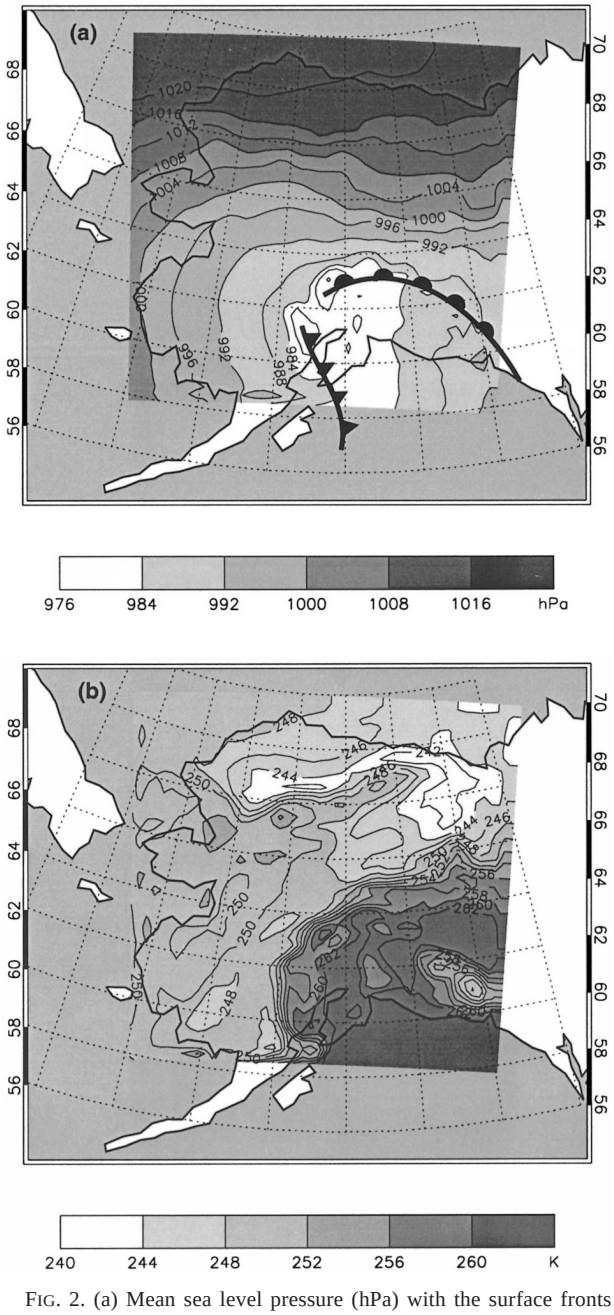

FIG. 2. (a) Mean sea level pressure (hPa) with the surface fronts and (b) boundary layer temperature (K, sigma level 18), on 21 Feb 1995, showing the passage of a front through the domain.

Typically, it is reasoned that climate is the ''ultimate ecological control'' (Sorensen 1977). Ritchie and Hare (1971) noted that the present-day Arctic front is located at a median of 300 km south of the tree line in most areas except Alaska and the Urals. These are areas of significant topography interacting with the tree line and with the prevailing flow, although Ritchie and Hare (1971) noted only the possibility of nonlinear feedbacks between vegetation, permafrost, soil, and the atmosphere to amplify ecosystem change. MacDonald et al. (1993) conducted a paeleoecological analysis of treeline vegetation and lakes during an episode of warming at the boreal tree line in central Canada 5000–4000 yr before present. The treeline advance was not found to coincide with the maximum in summer insolation, due to asynchronous shifts in the summer position of the Arctic front caused by small changes in frontal wave characteristics. More recently, MacDonald et al. (1998) note that the observed recent warming in this region

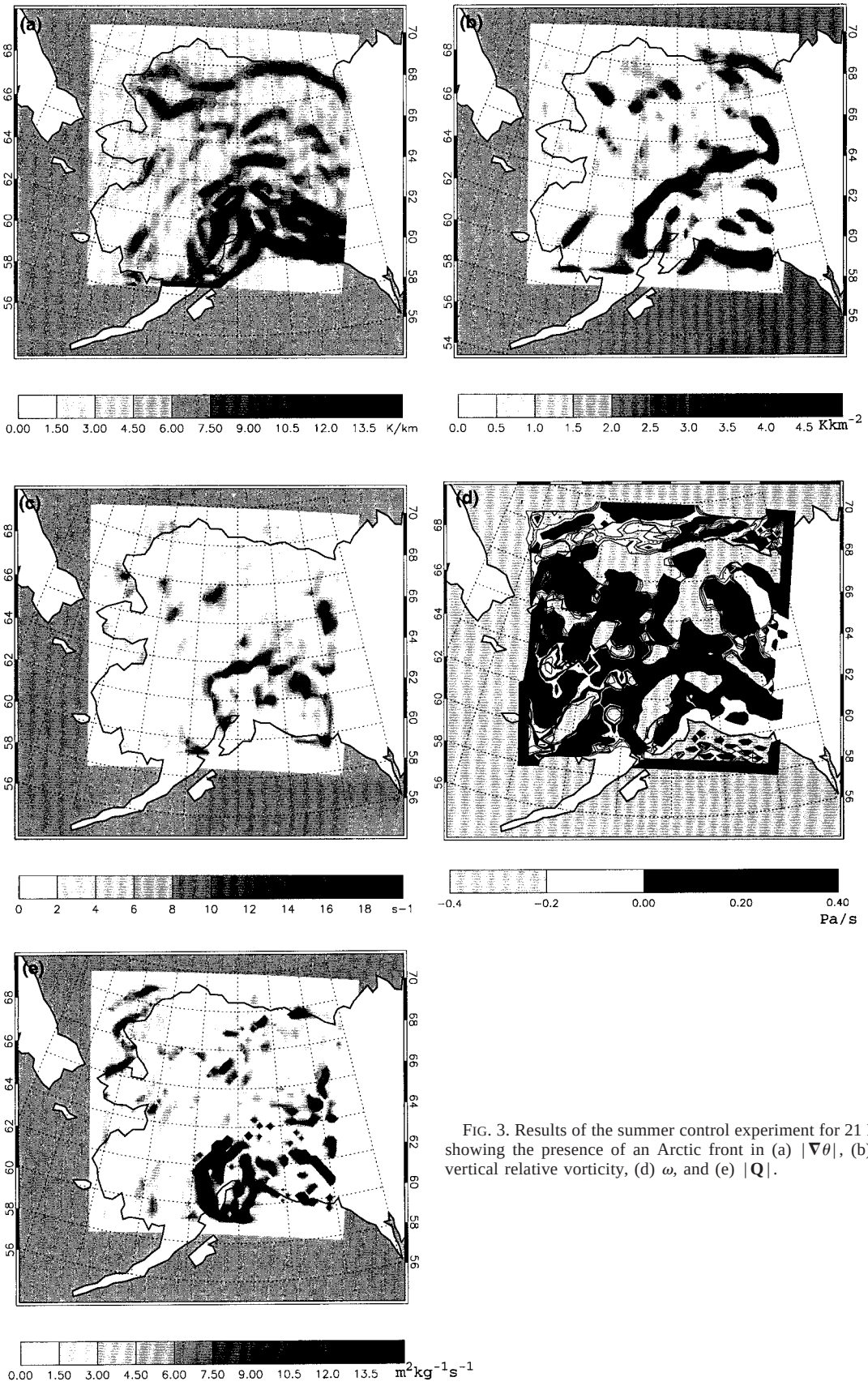

FIG. 3. Results of the summer control experiment for 21 Feb 1995, showing the presence of an Arctic front in (a) $|\nabla\theta|$, (b) TFP, (c) vertical relative vorticity, (d) ω, and (e) $|\mathbf{Q}|$.

TABLE 1. ARCSyM sensitivity tests.

Experiment	Configuration
Control	Annual cycle experiments for 1995 over the Alaskan domain and summer experiments for 1990 and 1998 over the western Arctic domain.
No ecotone	As for the control, but with all vegetation in the domain replaced by tundra, so that the treeline contrast is removed.
No mountains	As for the control, with the observed vegetation distribution, but with all land a uniform elevation of 1 m.
Coastal contrast	As for the control, but with uniform vegetation cover and uniform elevation, to test the efficacy of land–sea constraints alone in controlling the frontal zone.

does not coincide with significant northward treeline movement, but rather increased growth and higher rates of recruitment in treeline stands. Simulation of the response of latitudinal tree line to atmospheric warming suggest a 100–200-yr lag between atmospheric warming and tree line advance (Starfield and Chapin 1996; Chapin and Starfield 1997).

More recent studies, however, have more strongly emphasized vegetation controls on climate (e.g., Pielke and Vidale 1995; Chase et al. 2000; Fraedrich et al. 1999). The hypothesis of a treeline control on the Arctic frontal zone revolves around the argument that heat fluxes over the boreal forest are much larger than those over adjacent tundra, leading to a deeper and warmer boundary layer and hence the creation of large-scale horizontal thickness gradients between surface types. Using a geostrophic model, Pielke and Vidale (1995) used an estimated daily sensible heat contrast of 50 W m^{-2} inferred from the Boreal Ecosystem–Atmosphere Study (BOREAS) field program (Sellers et al. 1995) to show that this influence, if spread out over a distance of 500 km and distributed within the 1000–500-mb layer, would be sufficient to be classified as a synoptic front. Pielke and Vidale (1995) suggest that the difference in surface energy balance arises from the lower albedo of the forest. This leads to warmer temperatures, which are not compensated for by the larger transpiration of the forest (due to a larger leaf area index). Additional factors that could enhance sensible heat fluxes over the forest include its greater surface roughness, which increases the efficiency of turbulent energy exchanges, the shading of the surface that reduces ground heat flux (Chapin et al. 2000b), and the masking of snow in winter and particularly spring. Lynch et al. (1998) reported on the strong impact of spring snow masking on the relative surface energy balances of tundra and boreal forest.

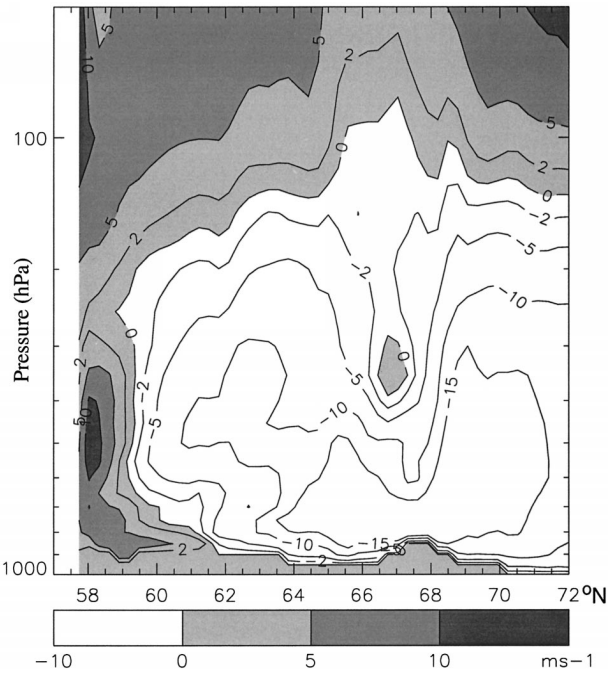

FIG. 4. The midtropospheric jet associated with the wintertime front on 21 Feb 1995 is clearly shown here in a north–south cross section of zonal wind with height.

Serreze et al. (2001) examined the expression of the Arctic frontal zone in the National Centers for Environmental Prediction–National Center for Atmospheric Research (NCEP–NCAR) reanalysis data over the period 1979–98 using a thermal front parameter [TFP; see section 2, Eq. (1)]. The analysis revealed a maximum in frontal frequencies over eastern Eurasia and Alaska in summer. This feature was easily distinguished from the polar front. It also corresponded to an upper-tropospheric jet, a preferred area for cyclogenesis, and to an area where the summertime contribution to annual precipitation is most dominant. The location and seasonality of the frontal zone were shown to be consistent with the effects of large-scale heating contrasts between the cold Arctic Ocean and snow-free land, and cold air damming by orography. While their conceptual model of frontal development does not require a treeline forc-

TABLE 2. Vegetation parameters for the different biomes for Aug. Albedo is calculated as the ratio of incoming to outgoing solar radiation. Roughness length and area indices are the weighted average of the plant/soil combinations that form each biome.

Biome type	Roughness length (m)	Total area index (m^2 m^{-2})	Leaf area index (m^2 m^{-2})	Albedo
Cool needleleaf evergreen tree	0.705 25	3.975	3.525	0.070
Cool broadleaf deciduous tree	0.825 25	3.6	2.550	0.071
Cool grassland	0.048 20	2.88	1.500	0.114
Tundra	0.036 40	1.65	0.810	0.199

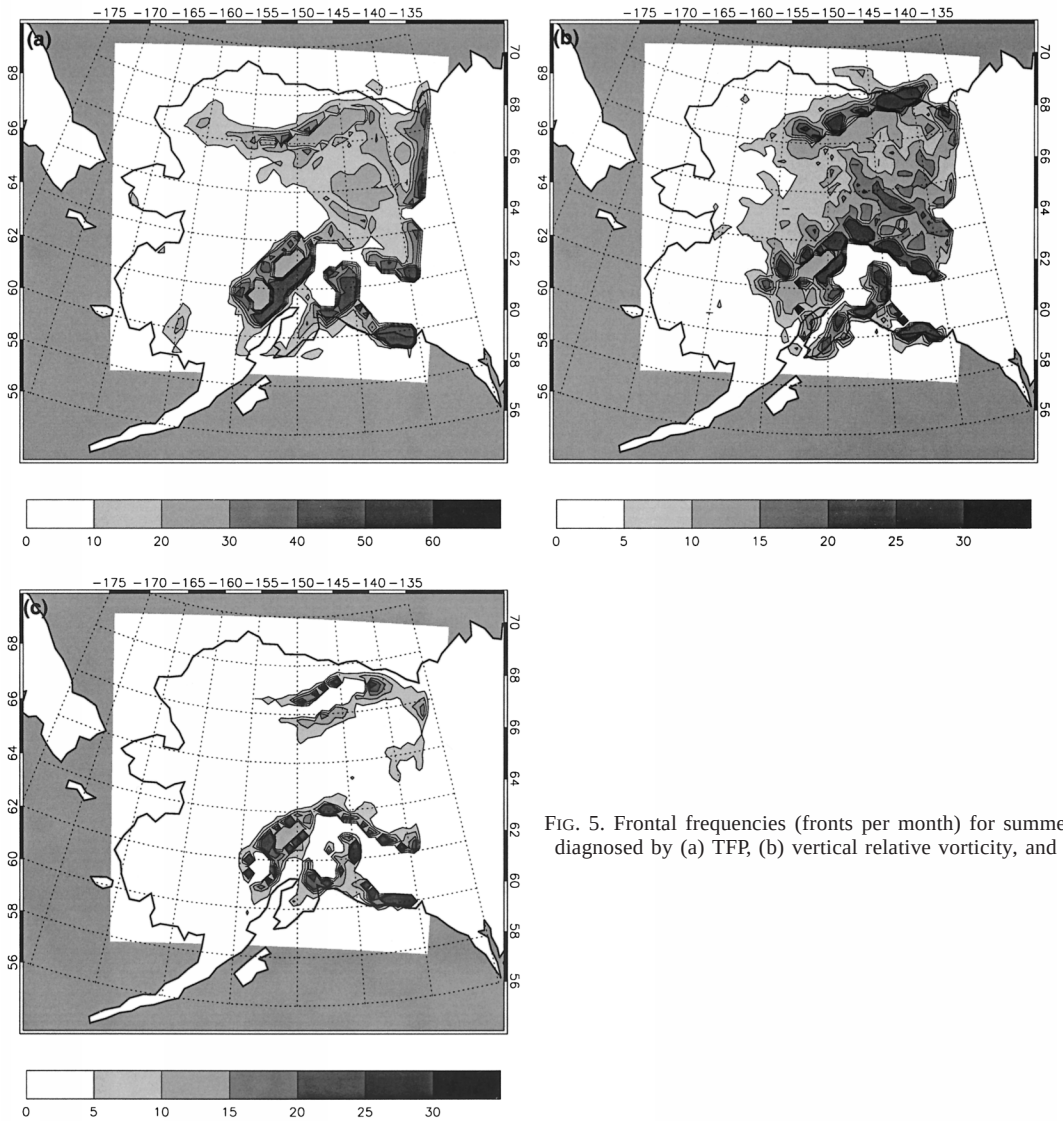

FIG. 5. Frontal frequencies (fronts per month) for summer 1995 as diagnosed by (a) TFP, (b) vertical relative vorticity, and (c) $|\mathbf{Q}|$.

ing, they note that such relationships might be masked by the low resolution of the analyses. Since the investigation of frontal seasonality by Serreze et al. (2001) indicated that the front was most strongly expressed during summer, if treeline control is the crucial aspect of Arctic front positioning, summer processes involving turbulent heat fluxes must be more important than the lowering of albedo by the masking of snow in spring. Further, additional heating of the forest in spring is not important for tree growth, and hence the potential for treeline movement and interactions between frontal position and the tree line must be sought in the summer season.

Summer measurements on the Seward Peninsula in Alaska (Beringer et al. 2000) found a sensible heat flux contrast of 60 W m^{-2} between forest and tundra in the 2 h either side of solar noon; however, the daily average differences were on the order of 10 W m^{-2}, 5 times smaller than the daily heating contrast proposed by Pielke and Vidale (1995). Similarly, measurements of treeline lichen woodland reveal average sensible heat fluxes only 12 W m^{-2} greater than tundra in eastern Canada (Lafleur et al. 1992). Moreover, shrub tundra, with the greatest sensible heat fluxes measured of all tundra types (Chapin et al. 2000b), is the vegetation type that most commonly adjoins boreal forest. Thus, depending upon where one draws the boundary between tundra and boreal forest, there can be as much variation in albedo and sensible heat fluxes *within* either boreal forest or tundra as *between* the two biomes (Eugster et al. 2000; Chapin et al. 2000a). Therefore, observations do not provide strong evidence for a significant and abrupt thermal contrast at the tree line in summer.

Bonan et al. (1992, 1995) used a global climate model to compare the effects of surface heating differences between boreal forest and tundra on the atmosphere. In

these experiments, the grid spacing was 2° × 2° in the land surface model and 4.5° latitude by 7.5° longitude in the atmospheric model. Bonan et al. (1992) compared the control simulation with one in which boreal forest was replaced by bare ground. While bare ground is not equivalent to tundra, the results with tundra (Bonan et al. 1995) were weaker but in the same direction. Surface albedo was found to be 0.3–0.4 higher in winter and spring in the bare ground simulation, as masking by the tree canopy is removed. The change in albedo was small (0.05) in summer. Air temperature at 2 m was found to be a few degrees lower in winter and summer in the bare ground simulation, but more than 10 K in spring. A 5-K temperature change corresponds to a thickness difference of 100 m in the 1000–500-mb layer, which although fairly small might contribute to frontal development. Bonan et al. (1992) note that the problem is strongly coupled and hence cannot be resolved by studying one component process. Foley et al. (1994) note that such large vegetation changes as those tested by Bonan et al. (1992, 1995) are unlikely to occur. Instead, Foley et al. (1994) take the approach of using paleoclimatic analysis to examine the response of climate to vegetation cover. Based on their global climate model experiments, they find that northward extension of boreal forests during the mid-Holocene resulted in a 4-K warming in spring due to lower albedo and a 1-K warming in other seasons. The average albedo change in summer is about 0.02, with an average increase in absorbed solar radiation of 7 W m^{-2} (highest in spring at 22 W m^{-2}). Hydrological changes are significant, however, with 5% increases in annual average precipitation with a more northward tree line, attended by decreased sea ice and snow cover. Levis et al. (1999) conducted a similar study examining future climate changes using a model with interactive vegetation, again noting the largest responses in spring, and warming of about 0.5 K in summer.

The objective of the present paper is to clarify the significance of vegetation boundaries on high-latitude frontal development in comparison with the influence of orography and coastal heating contrast. To this end we examine the results of sensitivity experiments conducted with the Arctic Regional Climate System Model (ARCSyM; Lynch et al. 1995, 1999) applied to Alaska where orography, vegetation boundaries, and coastal heating are well expressed. Section 2 describes the methods investigated for objective frontal diagnosis, section 3 presents the experimental design, and section 4 presents results from sensitivity experiments.

2. Frontal diagnosis

To objectively determine the occurrence of fronts in these simulations, a variety of thermally and dynamically based diagnostic tools were investigated (following McInnes et al. 1994). These include such measures of baroclinicity as the near-surface potential temperature gradient $|\nabla\theta|$ or the low-level thickness gradient $|\nabla(\Delta Z)|$ (Pielke and Vidale 1995), and a thermal front parameter (Serreze et al. 2001)

$$-\nabla|\nabla T_{850}|\cdot\mathbf{n}, \tag{1}$$

where T_{850} is the 850-hPa temperature and $\mathbf{n}$ is a unit vector in the direction of the 850-hPa temperature gradient. This parameter is a maximum where the temperature gradient is increasing most rapidly in the direction of an existing gradient. Fronts will be placed on the warm side of the baroclinic zones. The 850-hPa layer is chosen for consistency with Serreze et al. (2001) but is not required.

Dynamical measures include the vertical component of relative vorticity

$$\zeta = \frac{\partial v}{\partial x} - \frac{\partial u}{\partial y} \tag{2}$$

and measures of the vertical motion such as

$$\omega = -\sigma\left(\int_0^\sigma \nabla\cdot p_s u\, d\sigma + \mathbf{u}\cdot\nabla p_s\right). \tag{3}$$

The frontogenesis function (Hoskins 1982) combines these approaches as follows:

$$F_r = 2\mathbf{Q}\cdot\nabla_h\theta, \tag{4}$$

where the vertical levels are in σ coordinates, $\mathbf{u} = (u, v)$ is the horizontal wind on σ levels, θ is potential temperature, and p_s is the surface pressure. Here $\mathbf{Q}$ is proportional to the rate of change of the temperature gradient forced by the geostrophic wind, which can be most simply expressed in a coordinate system aligned locally with the isotherms:

$$\mathbf{Q} = -\frac{R}{p}\left|\frac{\partial T}{\partial y}\right|\mathbf{k}\times\frac{\partial\mathbf{u}}{\partial x}. \tag{5}$$

Since convergence of $\mathbf{Q}$ implies upward motion, this can be used in place of ω as a diagnostic tool in the objective identification of fronts. In addition, convergence of the low-level wind field is a good indication of vertical motion. Such measures of front location are not as complicated by stationary signals as thermal measures are, although topography still has a significant effect on diagnosis of regions of high baroclinicity, uplift, and cyclonic vorticity. Since these attributes, by any measure, constitute a dynamical front, we regard quasi-stationary signatures to constitute a viable part of the diagnosed fields. McInnes et al. (1994) note that the most unambiguous method of defining the position of a front in the presence of coastal and topographic variations is the axis of the relative cyclonic vorticity maximum. This is particularly true if advective rather than frontogenetic motion of the Arctic front is occurring.

3. Experimental design

In order to isolate the necessary and sufficient elements required to force the location of fronts, a series

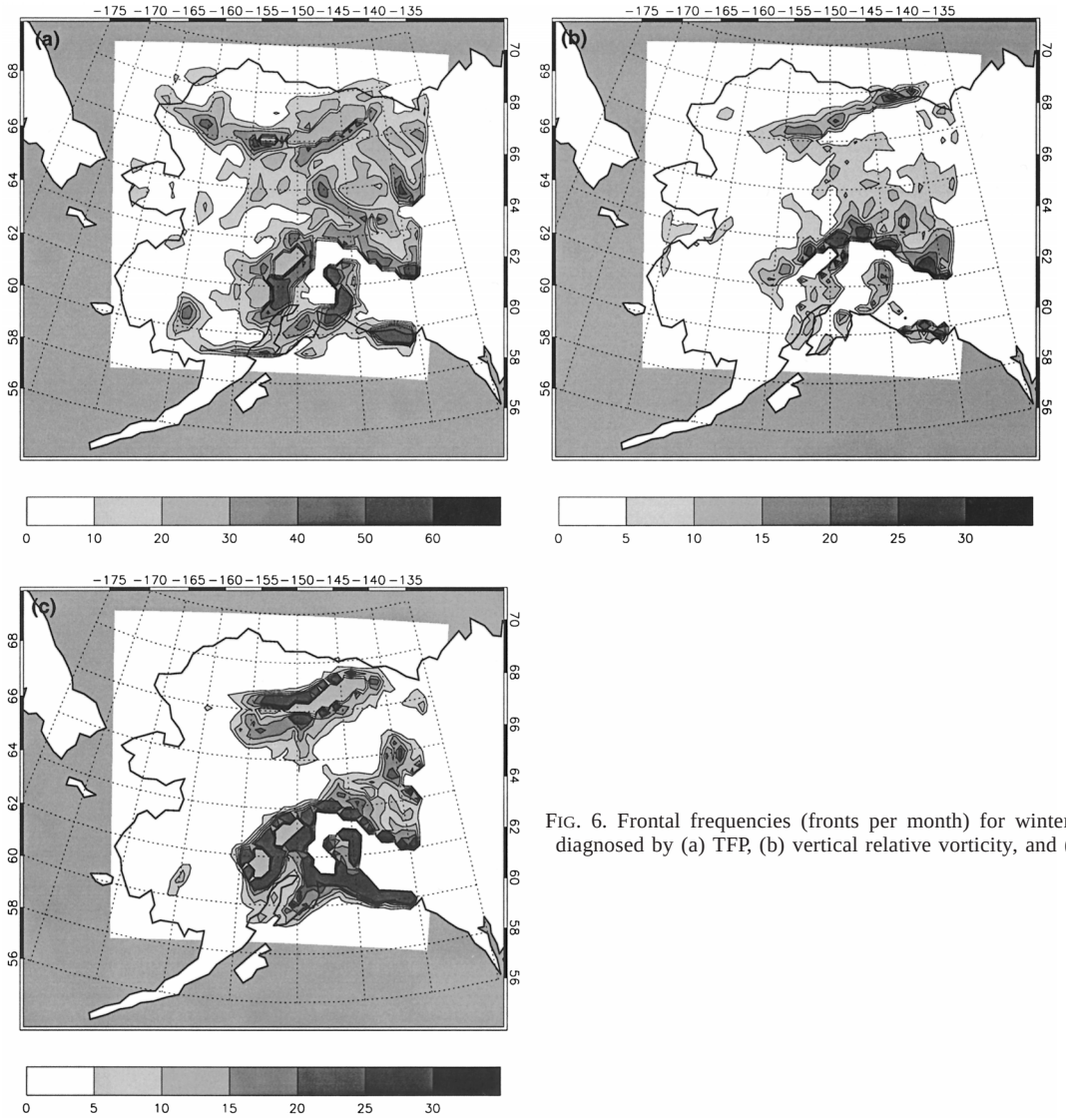

FIG. 6. Frontal frequencies (fronts per month) for winter 1995 as diagnosed by (a) TFP, (b) vertical relative vorticity, and (c) $|\mathbf{Q}|$.

of sensitivity tests was conducted using ARCSyM, a limited-area model that includes comprehensive treatments of the atmosphere, ocean, sea ice, and the land surface. The atmospheric component of the model includes physical parameterizations of convection and resolvable moist processes (Lynch et al. 1995), shortwave (Briegleb 1992) and longwave (Mlawer et al. 1997) radiation, and boundary layer processes (Holtslag et al. 1990). ARCSyM is forced at the lateral boundaries using temperature, wind, moisture, surface pressure, and height fields provided from the European Center for Medium-Range Weather Forecasts (ECMWF) operational analyses, which are updated every 12 h at every vertical level. The atmospheric component of ARCSyM is coupled to the NCAR Land Surface Model (Bonan 1996; Lynch et al. 1999). The sea ice is constrained to conform to derived ice area from the Special Sensor Microwave/Imager (SSM/I), with sea ice and lead temperatures calculated using the Parkinson and Washington (1979) ice thermodynamics, with modifications following Schramm et al. (1997). The model is configured over Alaska on a polar stereographic projection with a horizontal grid spacing of 30 km and 23 σ levels in the vertical (Fig. 1a). Lateral and upper boundary forcing is configured to prevent internal wave reflection (Lynch and Cullather 2000). The control model integration was initialized with prescribed conditions for 1 January 1995, using ECMWF analyses for the atmosphere, SSM/I sea-ice area and 1-m ice thickness, and January climatological mean land and ocean surface conditions. The model was then integrated for a 9-month period, thus providing a ''spunup'' initialization for the summer experiments, where soil moisture lags are more important than over winter. It should be noted that in this paper we are not comparing the model integrations with explicit observations (model validation); rather we are

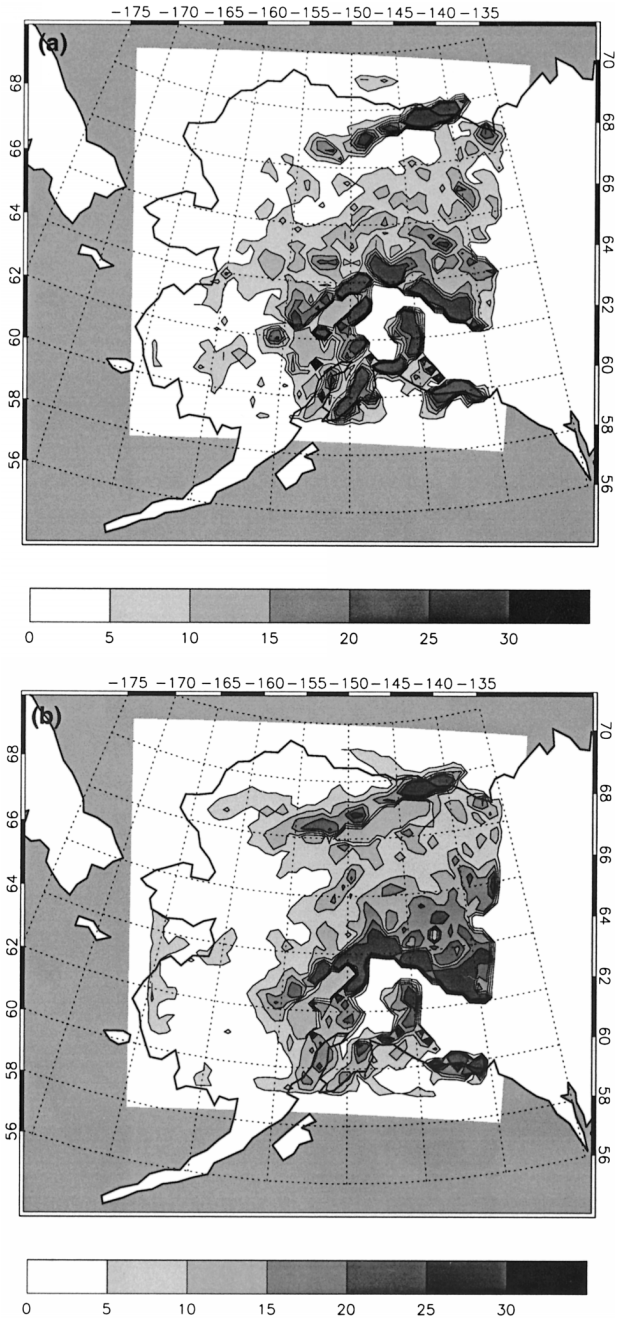

FIG. 7. Frontal frequencies (fronts per month) for (a) summer and (b) winter 1995 as diagnosed by the vertical relative vorticity, for the no-ecotone experiment.

looking at the differences in mechanisms simulated by the model, and thus issues of model initialization, spin-up, and interannual variability are not as critical as might be expected for validation purposes. Additionally, the timescales of atmospheric dynamic motions are short in comparison with surface/subsurface processes.

Four sets of simulations were undertaken (Table 1). A 9-month control simulation starting 1 January 1995, in which standard surface parameters and characteristics were assigned, was conducted as described above (Fig. 1b and Table 2). Pairs of 3-month sensitivity experiments used initial conditions from 1 January and 1 July of the control experiment for winter and summer, respectively. These included a ''no-ecotone'' experiment in which all vegetation points were specified with the characteristics of tundra, and a ''no-mountains'' experiment in which all land points were set to an altitude of 1 m. The atmospheric forcing data were interpolated from the original ECMWF analyses to the new (1 m) topography, thus ensuring temperatures and pressures were balanced on the model sigma levels at the boundaries. The final experiment, ''coastal contrast,'' was undertaken in which both uniform vegetation specification and uniform 1-m topography were combined to determine the impact of the land–sea contrast alone on frontal development.

4. Results

a. Comparison of frontal diagnostic tools for a particular summer case

A single case was first analyzed to determine the most useful tools for diagnosing frontal activity. Figure 2 shows the passage of a synoptic front on 21 February 1995 associated with an open wave cyclone that formed in the Gulf of Alaska and traversed central Alaska before moving into northwest Canada. The temperature field associated with the cyclone shown in Fig. 2b, reveals a pronounced warm sector impinging on the polar air mass with a strong cold front and warm front. Corresponding to this feature, Fig. 3 shows the magnitude of the gradient of near-surface potential temperature (at sigma level 18), the thermal front parameter (at 850 hPa), the magnitude of the vertical component of relative vorticity (at sigma level 21), ω (at sigma level 18), and $\mathbf{Q}$ (at sigma level 20). The thermal front parameter was calculated at 850 hPa to maintain consistency with the Serreze et al. (2001) study. The remaining diagnostics were computed at levels that generally showed features with great clarity—conclusions are not affected by this choice. All diagnostics are strongly affected by the extreme topography of the Alaska Range, which includes Mount McKinley, North America's tallest peak. In the smoothed model topography (Fig. 1), however, the maximum elevation is located farther east than the true position of Mount McKinley and is significantly lower than the true height (under 2700 m as compared with over 6000 m). The passage of synoptic cyclones is also strongly affected by the Brooks Range, with lee cyclogenesis playing an important role in the meteorological behavior of the region (Lynch 1997). Apart from this strong feature, all of the diagnostics pick up the propagating front to some degree. Regarding Figs. 2 and 3, it should be noted that the stationary signal of the topography could be filtered out, although the full fields

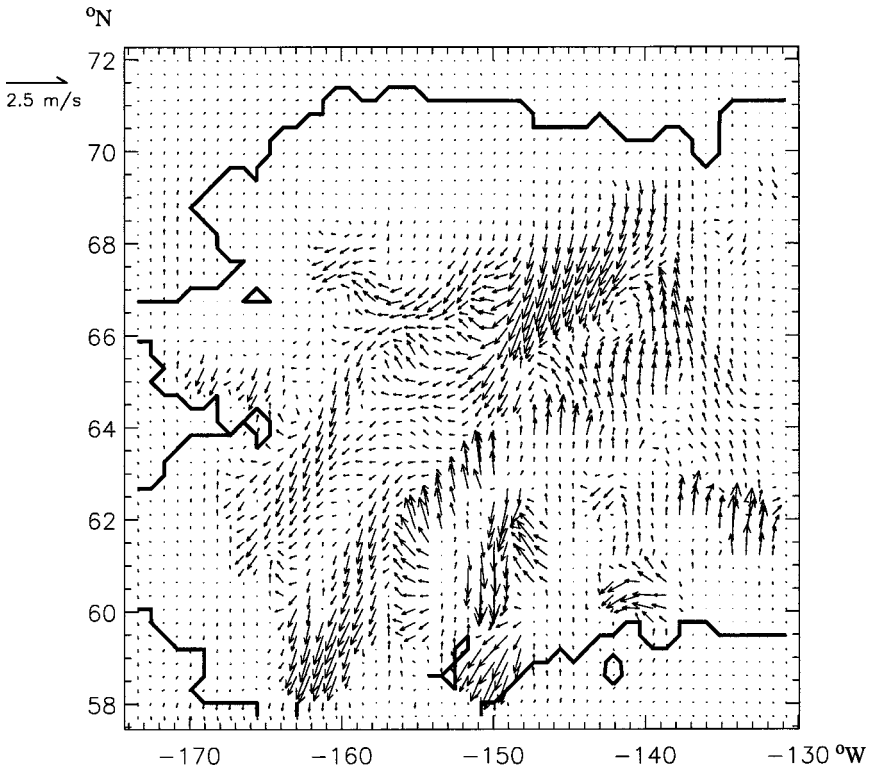

FIG. 8. Average surface wind differences for winter between the no-ecotone and control experiments. (Note vector scale located at top left of figure.)

are shown here for completeness. Vertical motion (Fig. 3d) is the most difficult field to interpret. As vertical velocities are small and highly subject to small errors in the horizontal divergence, this field is viewed as least useful. Similarly, the horizontal potential temperature gradient (Fig. 3a), while clearly showing the presence of the warm sector, is not very useful in identifying placements of the fronts themselves. By comparison, the TFP, vertical vorticity, and **Q** fields (Figs. 3b,c, and 3e) identify the fronts quite strongly; the **Q** field is the best indicator of the cold front location. Figure 4 shows the expected midtropospheric wind maximum (over 10 m s^{-1} at 500 hPa) above the position of the cold front in the southern part of the domain.

b. Frontal statistics for control experiment

Based on the example discussed above and inspection of results for additional cases, the TFP, vertical vorticity, and **Q** were selected as the most useful frontal diagnostics. Preferred frontal location in the simulations was hence defined in the ensuing manner. Following Serreze et al. (2001), the chosen diagnostics (TFP, vertical vorticity, and **Q**) were computed at 6-hourly intervals over the 3-month length of each simulation. If the magnitude of the diagnostic exceeded a threshold value at a particular grid location, it was assumed to indicate the presence of a front. The frequency of fronts at each grid location exceeding the threshold values was then determined on a seasonal basis. Last, purely stationary signals corresponding to topography and coastlines, indicated by a front occurring in the same location in every 6-hourly field, were removed. The threshold values for frontal identification are a matter of judgement. Serreze et al. (2001) used 1.0×10^3 K km^{-2} for the TFP, but this value was chosen to be appropriate for the 2.5° latitude–longitude grid spacing. Intensities of simulated fronts in a model are directly proportional to their horizontal resolution (Reeder and Smith 1988). However, given that our analyses are only over 3-month periods, we used the same threshold to highlight locations of preferred frontal activity. Results with a lower threshold were qualitatively the same as those shown here. Threshold values for vertical vorticity and **Q** were similarly derived by testing. Thus, the threshold for TFP is 1.0×10^3 K km^{-2}, for vertical vorticity it is 5.0 s^{-1}, and for **Q** it is 5.0 m^2 kg^{-1} s^{-1}. Using these threshold values, the frontal frequencies are shown in Fig. 5 for summer and Fig. 6 for winter. No attempt was made to separate specific frontal instances from one time period to the next, 6 h later, since the objective is to identify preferred locations of frontal position, not to conservatively identify specific synoptic frontal passages.

The summer Arctic frontal zone as reproduced by the regional model (Fig. 5) shows a similar pattern to that noted for the Alaskan region by Serreze et al. (2001).

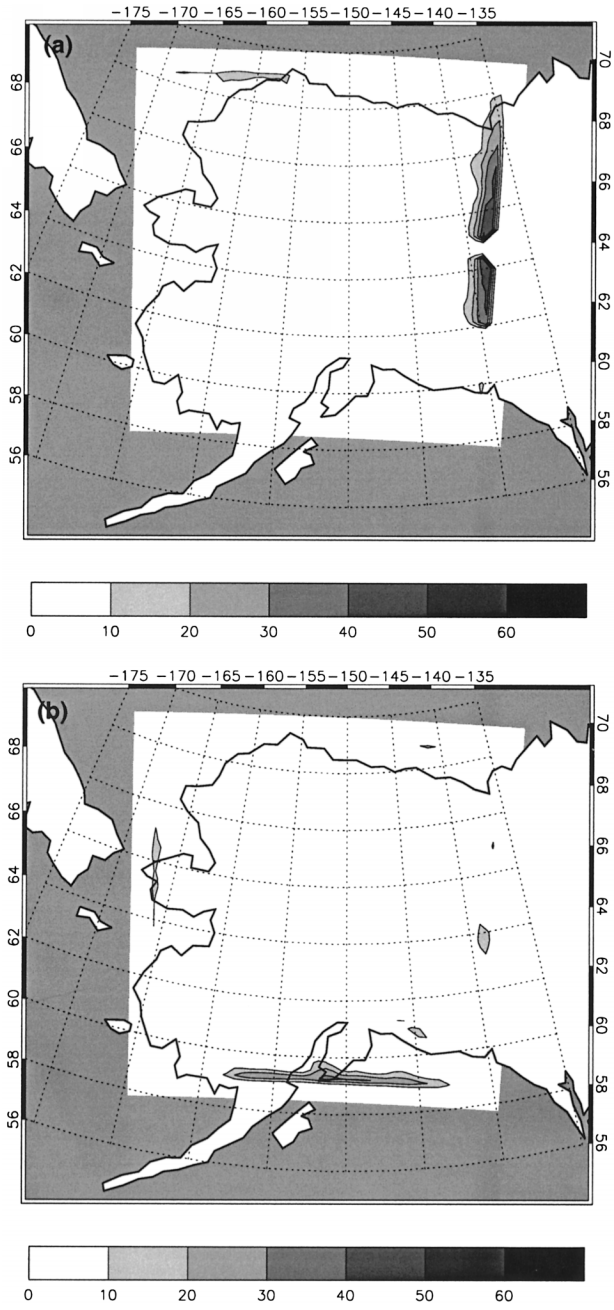

FIG. 9. Frontal frequencies (fronts per month) for (a) summer and (b) winter 1995 as diagnosed by the TFP, for the no-mountains experiment.

However, the higher resolution of the ARCSyM model allows the identification of two distinct zones of baroclinicity, cyclonic vorticity, and uplift, associated with the southern side of the eastern Brooks Range and the Alaska Range. The **Q** field is the most conservative frontal locator (recall that convergence of **Q** identifies regions of vertical motion), but it should be combined with the strong temperature gradients and cyclonic motion required to identify a dynamical front. The winter Arctic frontal zones (Fig. 6) show broader areas of high-frontal frequency, but in this season some activity is also indicated on the northern side of the Brooks Range, again clearly associated with leeside cyclogenesis. Frontal activity is clearly indicated in both the summer and winter seasons.

c. Sensitivity experiments

The uniform vegetation experiment denoted as no ecotone suggests that there is some control on frontal position related to the gradient in surface parameters associated with vegetation. The true gradient in vegetation is not as sharp as depicted in ARCSyM, in which the designations of vegetation are limited to generalized tussock tundra and boreal forest. The transition through shrub tundra and reduction in density of tree stands near the tree line are hence not expressed. Further, the tree line occurs abruptly at the boundary of large grid cells (Fig. 1). Hence, it would be expected that a larger response to the removal of the vegetation gradient would be observed in the model than in nature (Eugster et al. 2000; Beringer et al. 2000, 2001). Monthly frontal frequency of the above-threshold vertical component of cyclonic relative vorticity (as one example) from this experiment is shown in Fig. 7 for summer and winter. As can be seen by comparison with Figs. 5b and 6b, there is minimal observable change in the frontal frequencies diagnosed by this method, with one significant exception. There is a decrease in frontal frequency in summer in the treeline area south of the Brooks Range from 10–15 fronts per month to 0–5 fronts per month, corresponding to reduced heating gradient in this area. This mechanism points to a role in this region for the treeline heating gradient in summer frontal location. However, the regions of strongest frontal activity remain just south of the eastern Brooks Range and the Alaska Range area. In winter, there is a significant increase in frontal activity in the same area where a decrease is seen in the summer experiment, caused by stronger leeside cyclogenesis that appears to result from a reduced momentum exchange at the surface due to a decreased roughness length of vegetation (Lynch 1997). The resulting increase in the winds propagates upward from the surface through the planetary boundary layer and differences are most apparent at what was the ecotone in the control run (Fig. 8). Similar results are evident for the frontal frequencies diagnosed by the TFP and **Q** (not shown). Hence, the conclusion of Serreze et al. (2001) that the ecotone is not required in the theoretical model of the summertime Arctic front is generally supported by these results. However, this does not imply that the vegetation specification has no impact on the simulation—as noted, in the specific area of the tree line, summer frontal frequencies are diminished, and small differences in air temperature and circulation (not shown) are seen in the sensitivity experiment in response to the differing surface characteristics, consistent

with the conclusions of Lynch et al. (1999). Forested regions are generally cooler when replaced by tundra because of higher summer albedos in tundra, and very slight warming (within noise) is seen outside these areas. There is a tendency for increased northerly flow in the eastern part of the domain and in the Alaska Range, with more southerly flow in the Bering Strait and western Alaska areas. Areas of more anticyclonic motion are also reflected in the western Brooks Range vertical vorticity (Fig. 7a).

The no-mountains experiment (Fig. 9) shows much larger changes in frontal frequency. Only the TFP diagnostic is shown but the other diagnostics reveal the same response. In both summer and winter, the simulations with uniform topography show minimal cyclonic activity, little vertical motion, and, even with the tree line in place, weak lower-tropospheric baroclinicity. As a result, fewer than 10 fronts per month are identified across the domain. The features at the edges of the domain in this figure are artifacts of boundary relaxation and do not represent real features. It could be argued that many of the frontal regions identified in the control and no-ecotone experiment merely represent orographic features of cold mountain-top temperatures and lee cyclogenesis. However, since we have removed stationary features and then assumed that any lower-tropospheric baroclinic zone associated with uplift and cyclonic turning of the wind is a front, these orographically generated features are, by our definition, frontal features. The diagnostics also determine synoptic frontal passages (as shown in Fig. 3), and Fig. 9 shows no evidence of these features. Since frontal motion generally occurs by a process of frontogenesis ahead of the front and frontolysis behind the front, rather than simple advection (e.g., McInnes et al. 1994), this lack of fronts in the no-mountains experiment suggests a dominant role for the strong Alaskan topography in maintaining the passage of fronts from the Gulf of Alaska over the region. The final experiment, coastal contrast, omits the topographic and vegetation gradients in order to determine if coastal temperature contrasts alone may generate fronts using these diagnostics. A limitation of this experiment is the proximity of the boundary to the coastline. Not surprisingly, the results are largely similar to the no-mountains experiment, revealing fewer than 10 fronts per month within the domain that fit the criteria.

5. Conclusions

Various hypotheses have been put forward to explain the concurrence of the northern tree line and a distinct Arctic front. These include baroclinicity forced by a land–sea contrast, which in turn influences the tree line, or the tree line itself creating baroclinic conditions and frontal activity. In this paper we have investigated the mechanisms implicated in this phenomenon with the use of a regional climate system model in a series of experiments in which surface conditions were altered. While the experiments described here consider only a single year, so that interannual variability cannot be taken into account, the sensitivity of the model to the changes made provides a strong indication of the importance of these processes to preferred frontal locations. Further, it should be noted that smaller-scale processes at the tree line, associated with boundary layer convection and subgrid-scale vegetation distribution, cannot be assessed by this study.

It has been found that a combination of the vertical component of relative vorticity, a thermal front parameter, and the convergence of the **Q** vector creates a useful objective diagnostic for frontal activity, particularly if stationary features associated with topography and coastlines are filtered out. The scheme used in this study does not uniquely identify the passage of individual synoptic fronts but does identify preferred locations for the processes associated with frontal activity—cyclonic motion, surface baroclinicity, and ascent.

While vegetation does have an interdependence with the Arctic frontal zone, in those areas where topography exists, topography plays a considerably dominant role. The results noted here suggest that the vegetation contrast is insufficient to induce significant frontal activity, but can and will contribute to topographically generated preferred frontal zones. An interesting feature of the influence of vegetation is the winter response, when heating gradients associated with albedo and turbulent flux differences are at a minimum. During this season, the increased surface roughness of boreal forest is sufficient to reduce the instances of lee cyclogenesis that may be observed if downslope flow were associated instead with tundra.

It was noted in Serreze et al. (2001) that the coastal contrast played a significant role in the location of the frontal zone. The discrepancy between this conclusion and the results shown here is likely to be due to differences in horizontal grid spacing between the two studies. The grid spacing of the observational analyses employed by Serreze et al. (2001), especially when reduced by the calculation of the thermal front parameter, is too large to resolve the closely juxtaposed Brooks Range and Beaufort Sea coast. Further, the baroclinicity detected in the analyses must necessarily be of larger scale than the synoptic and subsynoptic-scale frontal activity diagnosed in this study.

The Alaskan region is characterized by a particular configuration of vegetation distribution, topography, and coastline that makes it a prime candidate for this type of modeling study. Since the elevation changes of the Brooks Range strongly influences the location of the tree line, and the coastline and Brooks Range are closely parallel for much of their extent, an observational study cannot distinguish the confounding factors that influence frontal location. However, such a configuration also means that while the conclusions associated with mechanisms are generally applicable, the particular diagnoses of preferred frontal location must be peculiar

to this region. A natural extension of this work will be to expand the analysis to the full Arctic Basin.

Acknowledgments. Thanks to Terry Chapin and Jason Beringer for access to their data and for discussions concerning the Arctic front, and to Roger Pielke Sr. for useful comments at the LAII annual meeting. We appreciate the comments of two anonymous reviewers. This work was supported by NSF Grant OPP-9732461 and NASA Grant NAG5-6820.

REFERENCES

Barry, R. G., 1967: Seasonal location of the Arctic front over North America. *Geogr. Bull.,* **9,** 79–95.

Beringer, J., F. S. Chapin III, I. McHugh, and N. J. Tapper, 2000: Observations on the role of treeline in controlling atmospheric circulations. Preprints, *24th Conf. on Agricultural and Forest Meteorology,* Davis, CA, Amer. Meteor. Soc., 93–94.

——, ——, ——, ——, A. H. Lynch, M. C. Serreze, and A. G. Slater, 2001: Impact of Arctic treeline on synoptic climate. *Geophys. Res. Lett.,* in press.

Bonan, G. B., 1996: A Land Surface Model (LSM version 1.0) for ecological, hydrological, and atmospheric studies: Technical description and users's guide. NCAR Tech. Note TN-417+STR, 150 pp.

——, D. Pollard, and S. L. Thompson, 1992: Effects of boreal forest vegetation on global climate. *Nature,* **359,** 716–718.

——, F. S. Chapin III, and S. L. Thompson, 1995: Boreal forest and tundra ecosystems as components of the climate system. *Climatic Change,* **29,** 145–167.

Briegleb, B. P., 1992: Delta-Eddington approximation for solar radiation in the NCAR Community Climate Model. *J. Geophys. Res.,* **97,** 7603–7612.

Bryson, R. A., 1966: Air masses, stream lines and the boreal forest. *Geogr. Bull.,* **8,** 228–269.

Chapin, F. S., III, and A. M. Starfield, 1997: Time lags and novel ecosystems in response to transient climatic change in Arctic Alaska. *Climatic Change,* **35,** 449–461.

——, W. Eugster, J. P. McFadden, A. H. Lynch, and D. A. Walker, 2000a: Summer differences among arctic ecosystems in regional climate forcing. *J. Climate,* **13,** 2002–2010.

——, and Coauthors, 2000b: Arctic and boreal ecosystems of western North America as components of the climate system. *Global Change Biol.,* **6,** 211–223.

Chase, T. N., R. A. Pielke, T. G. F. Kittel, R. R. Nemani, and S. W. Running, 2000: Simulated impacts of historical land cover changes on global climate in northern winter. *Climate Dyn.,* **16,** 93–105.

Dzerdzeevskii, B. L., 1945: Tsirkuliatsionnye skhemy v troposfere. *Tsentral' noi Arktiki. Izdatel' svo Akad. Nauk.* [English translation: UCLA Sci. Rep. 3, Contract AF 19(122)-3228.]

Eugster, W., and Coauthors, 2000: Land–atmosphere energy exchange in Arctic tundra and boreal forest: Available data and feedbacks to climate. *Global Change Biol.,* **6** (Suppl.), 84–115.

Foley, J. A., J. E. Kutzbach, M. T. Coe, and S. Levis, 1994: Feedbacks between climate and boreal forests during the Holocene epoch. *Nature,* **371,** 52–54.

Fraedrich, K., A. Kleidon, and F. Lunkeit, 1999: A green planet versus a desert world: Estimating the effect of vegetation extremes on the atmosphere. *J. Climate,* **12,** 3156–3163.

Hare, F. K., and J. C. Ritchie, 1972: The boreal microclimates. *Geogr. Rev.,* **62,** 333–365.

Holtslag, A. A. M., E. I. F. de Bruijn, and H. L. Pan, 1990: A high resolution air mass transformation model for short-range weather forecasting. *Mon Wea. Rev.,* **118,** 1561–1575.

Hoskins, B. J., 1982: The mathematical theory of frontogenesis. *Annu. Rev. Fluid. Mech.,* **14,** 131–151.

Lafleur, P. M., W. R. Rouse, and D. W. Carlson, 1992: Energy balance differences and hydrologic impacts across the northern treeline. *Int. J. Climatol.,* **12,** 193–203.

Levis, S., J. A. Foley, and D. Pollard, 1999: Potential high-latitude vegetation feedbacks on CO_2-induced climate change. *Geophys. Res. Lett.,* **26,** 747–750.

Lynch, A. H., 1997: Topographically generated gravity waves in the Brooks Range, Alaska. *Geophys. Res. Lett.,* **24,** 2981–2984.

——, and R. I. Cullather, 2000: An investigation of boundary forcing sensitivities in a regional climate model. *J. Geophys. Res.,* **105,** 26 603–26 617.

——, W. L. Chapman, J. E. Walsh, and G. Weller, 1995: Development of a regional climate model of the western Arctic. *J. Climate,* **8,** 1555–1570.

——, D. L. McGinnis, and D. A. Bailey, 1998: Snow–albedo feedback and the spring transition in a regional climate system model: Influence of land surface model. *J. Geophys. Res.,* **103,** 29 037–29 049.

——, G. B. Bonan, F. S. Chapin III, and W. Wu, 1999: The impact of tundra ecosystems on the surface energy budget and climate of Alaska. *J. Geophys. Res.,* **104,** 6647–6660.

MacDonald, G. M., T. W. D. Edwards, K. A. Moser, R. Pienitz, and J. P. Smol, 1993: Rapid response of treeline vegetation and lakes to past climate warming. *Nature,* **361,** 243–246.

——, J. M. Szeicz, J. Claricoates, and K. A. Dale, 1998: Response of the central Canadian treeline to recent climatic changes. *Ann. Amer. Assoc. Geogr.,* **88,** 183–208.

McInnes, K. L., J. J. McBride, and L. M. Leslie, 1994: Cold fronts over southeastern Australia: Their representation in an operational numerical weather prediction model. *Wea. Forecasting,* **9,** 384–409.

Mlawer, E. J., S. J. Taubman, P. D. Brown, M. J. Iacono, and S. A. Clough, 1997: Radiative transfer for inhomogeneous atmospheres: RRTM, a validated correlated-*k* model for the longwave. *J. Geophys. Res.,* **102,** 16 663–16 682.

Parkinson, C. L., and W. M. Washington, 1979: A large-scale numerical model of sea-ice. *J. Geophys. Res.,* **84,** 311–337.

Pielke, R. A., and P. L. Vidale, 1995: The boreal forest and the polar front. *J. Geophys. Res.,* **100,** 25 755–25 758.

Reed, R. J., and B. A. Kunkel, 1960: The Arctic circulation in summer. *J. Meteor.,* **17,** 489–506.

Reeder, M. J., and R. K. Smith, 1988: On the horizontal resolution of fronts in numerical weather prediction models. *Aust. Meteor. Mag.,* **36,** 11–16.

Ritchie, J. C., and F. K. Hare, 1971: Late-quaternary vegetation and climate near the Arctic tree line of northwestern North America. *Quat. Res.,* **1,** 331–341.

Schramm, J. L., M. M. Holland, J. A. Curry, and E. E. Ebert, 1997: Modeling the thermodynamics of a sea ice thickness distribution. Part 1: Sensitivity to ice thickness resolution. *J. Geophys. Res.,* **102,** 23 079–23 091.

Sellers, P., and Coauthors, 1995: The Boreal Ecosystem–Atmosphere Study (BOREAS): An overview and early results from the 1994 field year. *Bull. Amer. Meteor. Soc.,* **76,** 1549–1577.

Serreze, M. C., A. H. Lynch, and M. P. Clark, 2001: The summer Arctic frontal zone as seen in the NCEP–NCAR reanalysis. *J. Climate,* **14,** 1550–1567.

Sorenson, C. J., 1997: Reconstructed Holocene bioclimates. *Ann. Amer. Assoc. Geogr.,* **67,** 214–222.

Starfield, A. M., and F. S. Chapin III, 1996: Model of transient changes in Arctic and boreal vegetation in response to climate and land use change. *Ecol. Appl.,* **6,** 842–864.